PAPER *Special Issue on Recent Progress in Microwave and Millimeter-wave Photonics Technologies*

An Experimental Investigation of Interference Suppression in Direct Optical Switching CDM Radio-on-Fiber System

Takeshi HIGASHINO[†a)], ***Student Member***, **Katsutoshi TSUKAMOTO**[†], ***Regular Member***, ***and*** **Shozo KOMAKI**[†], ***Fellow***

SUMMARY This paper describes the experimental approach of the Direct Optical Switching (DOS) CDM Radio-on-Fiber (RoF) system. Improved carrier-to-interference ratio (CIR) performance by using an Optical Polarity Reversing Correlator (OPRC) in comparison to using a single switch decoder is experimentally obtained. In addition, CIR performance deterioration due to degradation of the extinction ratio of the optical switch decoder is clarified from the theoretical and experimental viewpoints. Finally, we confirmed that CIR performance is improved more by using an M-sequence whose weight is even numbered than by using an odd numbered one.

key words: *microwave photonics, radio on fiber, CDM, interference suppression, optical polarity reversing correlator*

1. Introduction

Microwave Photonics technologies enable us to open a free space link for radio signals in optical fiber. On the basis of the virtual radio free space networking concept, we have proposed and studied the Radio-on-Fiber (RoF) network (Radio Highway) [1], where radio signals from terminals are transmitted to a remote Control Station (CS) or other cells through photonic routing switches without any demodulation, and all complicated functions are performed at a CS. A radio base station (RBS) is only equipped with E/O (electric-to-optic) and O/E (optic-to-electric) converters. As the configuration for the RoF system, the bus type or passive double star optical link is desirable from the viewpoint of low cost implementation and easy addition of access points. As a multiple access method for the RoF system, we have proposed the TDMA [2], [3] and CDMA [4] methods by using a Direct Optical Switching (DOS) technique [5] which performs on-off switching at the optical switch. While the TDMA method requires time synchronization among whole RBSs, the CDMA method has many advantages, such as its asynchronous accessibility, flexibility and transparency for radio air interfaces. Furthermore, the optical CDMA scheme is more suitable for the RoF system than conventional electrical CDMA schemes because a higher process gain can be obtained by using the broadband photonic devices when RF signals are multiplexed in the optical domain.

The DOS CDM system can employ the M-sequence and Gold sequence which are used in conventional radio systems by employing the Optical Polarity Reversing Correlator (OPRC) [6]. In this work, we use the M-sequence as a code for multiplexing. In the DOS CDM system, a M-sequence is mapped into an optical on-off intensity pulse sequence and at the OPRC receiver, two optical switches and a balanced mixing PD perform de-spreading. Since the M-sequence and Gold-sequence are generally superior in terms of distinct code numbers, OPRC can improve its capacity. Moreover, since the number of '1's within a code period is about one-half of the code length, the carrier-to-noise ratio (CNR) can also be improved compared to using the optical orthogonal codes (OOC) such as prime codes. The principle of interference suppression using OPRC in the DOS CDM RoF system was studied and experimentally demonstrated [7], [9], [10]. This paper shows the experimental investigation of CIR performance in the DOS CDM RoF system. We obtained the improved CIR performance experimentally by using an OPRC in comparison to using a single switch decoder. In addition, CIR performance deteriorates with degradation of the extinction ratio of the optical switch. Therefore we also investigated the CIR performance deterioration experimentally. Furthermore, we observed that the CIR performance is improved more by using an even weight M-sequence than by using an odd weight M-sequence in the DOS CDM RoF system.

The paper is organized as follows. In Sect. 2 we show the configuration of the DOS CDM RoF system. In Sect. 3 we show the interference suppression experiment and experimental results. In Sect. 4 we discuss the CIR degradation factor. In Sect. 5 we show CIR improvement method using OPRC and the experimental results of measured CIR performance. Section 6 concludes this paper.

2. Configuration of DOS CDM Radio on Fiber System

Figure 1 shows the configuration of the DOS CDM RoF system. The DOS scheme can be realized by optical switching. An optical carrier intensity modulated by

Manuscript received December 2, 2002.
Manuscript revised February 12, 2003.

[†]The authors are with the Department of Communications Engineering, Graduate School of Engineering, Osaka University, Suita-shi, 565–0871 Japan.
a) E-mail: higa@roms.comm.eng.osaka-u.ac.jp

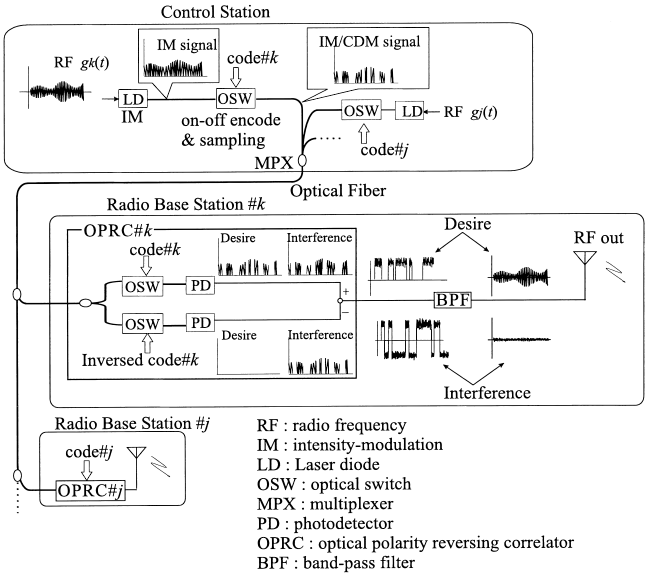

Fig. 1 Configuration of DOS CDM system.

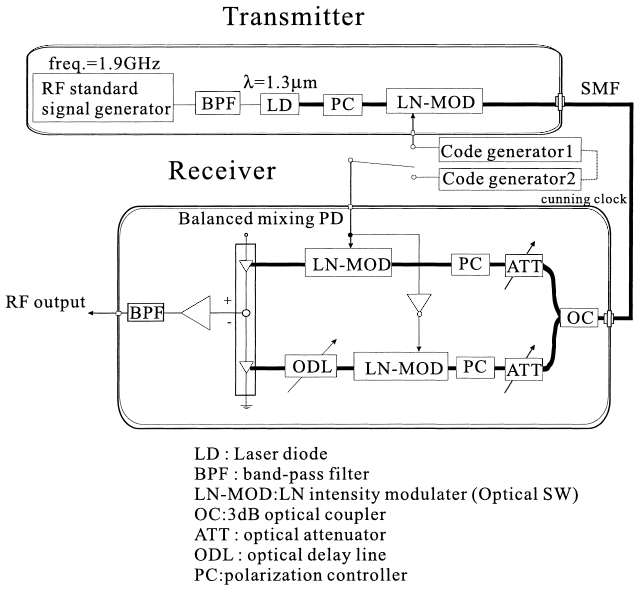

Fig. 2 Experimental setup.

the RF signal is transmited from CS to each RBS via the downlink. The IM signal is on-off encoded at the optical switch (OSW) driven by an M-sequence. This on-off switching is equivalent to sampling of the RF signal. Since the RF signal is a bandpass signal, the sampling code rate requires more than twice the bandwidth of the RF signal. M IM/CDM signals are multiplexed at the output of CS and transferred to each RBS. At the RBS, IM/CDM signals are correlated in the optical domain at OPRC. At the OPRC, the two OSWs of the upper side and lower side branches are driven with '1' and '0' symbols of the de-spreading M-sequence which is identical to a desired RF signal. As a result, the PD output current of the upper side branch is the sum of the desired signal and the interference signals when OSW is driven with the desired code, and the PD output current of the lower side branch includes only the interference signals. The output of OPRC is obtained by the subtraction of the lower branch's signal from the upper branch's signal. Thus, we obtain the desired RF signal contaminated with some reduced-power interference RF signals. At this stage, the desired signal is still an on-off pulsed signal. Therefore, in order to obtain the original RF signal, we finally interpolate it by using a band-pass filter (BPF).

3. Experiment of Interference Suppression

3.1 Experimental Setup

Figure 2 and Table 1 show the experimental setup and a summary of the specifications of devices, respectively. The transmitter consists of Laser Diode (LD) and a $LiNbO_3$ intensity modulator (LN-MOD). The RF signal, generated from the signal generator, intensity modulates the LD with its wavelength of 1.3 μm. The IM signal is on-off encoded by the LN modulator driven with the rectangular pulsed M-sequence from an arbitrary waveform code generator.

Table 1 Specifications of devices used in experiments.

LD module (ORTEL 3541C)	DFB Laser wavelength λ:1.3 μm output power:3.4 dBm RIN:-149 dB/Hz sensitivity γ:0.103W/A
LN modulator (transmitter) (SumitomoTMZ1.3-2.5)	insertion loss:5.4 dB extinction ratio=33 dB half-wave voltage V_π:2 V
LN modulator (receiver) (RAMAR corp.)	insertion loss:6.6 dB, 20.0 dB extinction ratio>28 dB V_π:8.5V,15V
PD(NEC NDL5481P1)	sensitivity:0.91 [A/W]
RF modulation method	$\pi/4$ shift DQPSK
RF carrier frequency	1.9 [GHz]
input RF power	10 [dBm]
chip rate of M-seq.	70 [kcps]–20 [Mcps]
code length	7-2047
bandwidth of RF signal	300 [kHz]

The receiver consists of a 3 dB coupler, two LN modulators (LN-MOD), an optical delay line (ODL), two optical attenuators (ATT), a balanced mixing PD (BMPD), a band-pass filter (BPF), and an RF amplifier. At the receiver, the received optical signal is divided into two branches by the 3 dB coupler. The divided optical signals are decoded by each LN-MOD. The lower side LN-MOD is driven with an inversed input M-sequence. At the BMPD, the decoded optical signals are photodetected and subtracted. Then, the desired RF signal is regenerated from the pulsed RF signal and the interference signal is suppressed by interpolation at the BPF. In this experiment, we use an

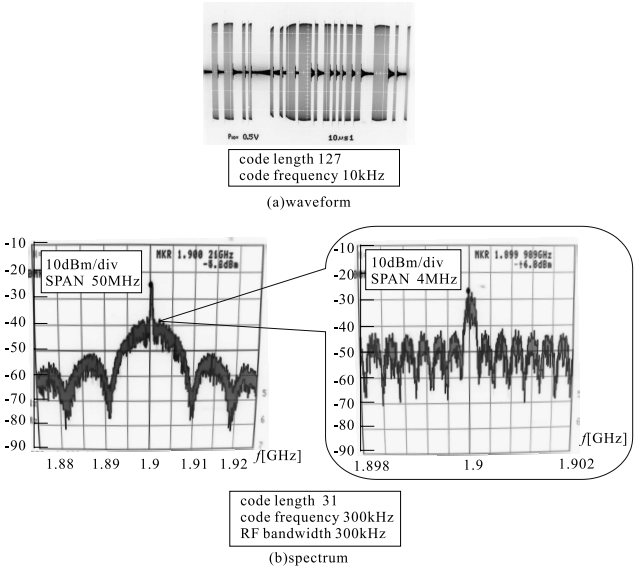

Fig. 3 Waveform and spectrum of a transmitter output.

optical delay line in order to balance the light path length of both branches. We also use an optical attenuator in order to balance the optical power of both branches.

3.2 Exprimental Results of Interference Suppression

Figure 3(a) shows an example of output waveform of the transmitter output in the case of the code length of 127 and code frequency of 10 kHz. We can see that the PN pattern is mapped into RF intensity-modulating signal. Figure 3(b) shows an example of the spectrum of the transmitter output in the case that code length is 31 and chip rate is 9 Mcps. The spectrum becomes symmetric sinc type about the center frequency of 1.9 GHz. In this figure, the bandwidth of the RF signal is 300 kHz, and the harmonic components appear at intervals of the code frequency, 300 kHz. Furthermore, the spectrum zero point appears at the interval of the chip rate.

The receiver output RF signal power was observed by means of a spectrum analyzer. The desired RF signal power is measured when the transmitter and the receiver use the same M-sequence. Code synchronization between the transmitter and receiver is obtained by using a clock. On the other hand, the interference RF power is measured when the receiver uses the bit-shifted M-sequence. Thus, we evaluate the interference RF signal power.

Figure 4 shows the spectrum, space diagram and eye pattern of the received, desired and interference RF signals. In the case that the chip rate of the M-sequence is 310 kcps, we obtained approximately 15 dB CIR. From the space diagram and eye pattern, it is evident that the desired RF signal is normally demodulated, but the interference RF signal cannot be demodulated. This experimental result shows that an interference suppression effect of the OPRC is obtained.

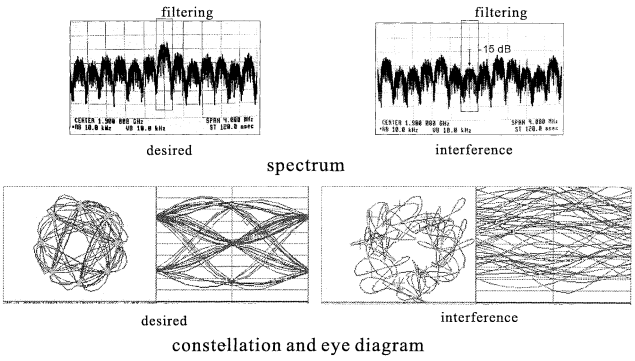

Fig. 4 Spectrum, space diagram and eye pattern of received desired RF signal and interference.

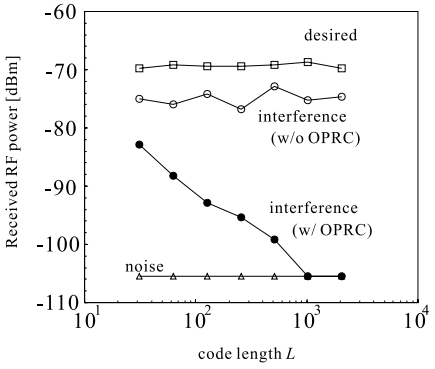

Fig. 5 Experimental result for received RF power.

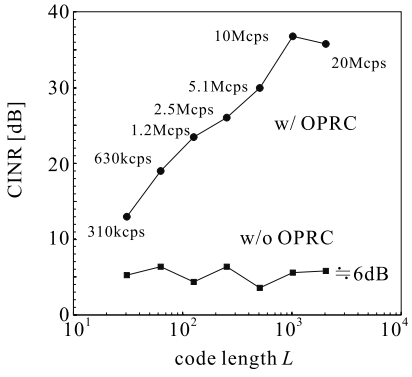

Fig. 6 CINR versus code length.

Figure 5 shows the received RF power of the desired signal, interference and noise versus code length L, when the transmitted RF signal is a non-modulated carrier wave (1.9 GHz) and the code period is fixed to 0.1 msec. In the figure, the interference suppression effect of using the OPRC is increased as the code length is increased in comparison to using a single switch decoder.

Figure 6 shows the CINR performance as calculated from Fig. 5. The parameter presented in this figure shows the chip rate in the measurement. The CINR

is defined as the received radio signal power ratio of desired signal and interference signal plus noise. In the figure, the OPRC can improve CINR as the code length is increased. For example, 13 dB CINR is obtained in the case that code length is 31 chips, and 35 dB CINR is obtained in the case that code length is 1023 chips. On the other hand, the CINR performance was not dependent on the code length and its value was around 6 dB.

4. Discussion of CIR Degradation Factor

In this section, we discuss the CIR deterioration factor from the experimental and theoretical viewpoints. This theoretical analysis includes the extinction ratio, insertion loss of the optical switch decoder and the sensitivity of BMPD. Let r_t, r_1, r_2 denote the extinction ratio of the transmitter's optical switch and these of the two optical switches used on the receiver's upper side, and lower side, respectively. The extinction ratio of the optical switch is defined as the optical power ratio of On-pulse to Off-pulse. We assume that the insertion losses of the upper side and lower side optical switches are l_1 and l_2, and the sensitivities of the upper side PD and lower side PD are α_1 and α_2, respectively. For the received desired signal, the PD output current of upper side branch, i_{Co1}, and lower side branch, i_{Co2}, are given by

$$i_{Co1} = m\frac{\alpha_1}{l_1}\left(L_{c1} + r_t r_1 L_{c2}\right) P_r, \tag{1}$$

$$i_{Co2} = m\frac{\alpha_2}{l_2}\left(r_2 L_{c1} + r_t L_{c2}\right) P_r, \tag{2}$$

where m is the intensity modulation index at LD, and P_r is the average optical received power. L_{c1} is the pulse number ratio within a code length which is passed through the upper side optical switch and L_{c2} is the pulse number ratio within a code length which is suppressed by the upper side optical switch. These number ratios depend on the kind of spreading code and code length. If using an M-sequence whose length is L and whose weight is an odd number as a code for multiplexing, L_{c1} and L_{c2} are given by $\frac{L-1}{2L}$ and $\frac{L+1}{2L}$, respectively. Let η_1, η_2, and $\Delta\eta$ denote α_1/l_1, α_2/l_2 and η_2/η_1, respectively. From Eqs. (1) and (2), we can derive the desired RF power, C_{odd}, in the case of using an M-sequence with its odd weight by

$$C_{odd} = \frac{1}{2}\left[mP_r\eta_1\left\{(1 - r_2\Delta\eta)\frac{L-1}{2L} + r_t\left(r_1 - \Delta\eta\right)\frac{L+1}{2L}\right\}\right]^2 \cdot \frac{RG}{4}, \tag{3}$$

where G is the total RF amplification gain after photodetection, and R is the receiver load impedance.

For an interference signal, correspondingly, the PD output currents of the upper side branch, i_{Io1}, and the lower side branch, i_{Io2}, are given by

$$i_{Io1} = m\frac{\alpha_1}{l_1}\left(L_{I1} + r_1 L_{I2} + r_t L_{I3} + r_t r_1 L_{I4}\right) P_r, \tag{4}$$

$$i_{Io2} = m\frac{\alpha_2}{l_2}\left(r_2 L_{I1} + L_{I2} + r_t r_2 L_{I3} + r_t L_{I4}\right) P_r, \tag{5}$$

where L_{I1} is the pulse number ratio within a code length after passing through the upper side optical switch. L_{I2} is the pulse number ratio within a code length suppressed by the upper side optical switch. L_{I3} is the pulse number ratio within a code length suppressed by the transmitter's optical switch. L_{I4} is the pulse number ratio within a code length suppressed by the transmitter's optical switch and the receiver's upper side optical switch. Therefore, L_{I1}, L_{I2}, L_{I3} and L_{I4} are given by $\frac{L+1}{4L}$, $\frac{L-3}{4L}$, $\frac{L+1}{4L}$ and $\frac{L+1}{4L}$, respectively. From Eqs. (4) and (5), we can derive the interference RF power, I_{odd}, by

$$I_{odd} = \frac{1}{2}\left[mP_r\eta_1\left\{(1-r_2\Delta\eta)\frac{L+1}{4L} + (r_1-\Delta\eta)\frac{L-3}{4L} + r_t(1-r_2\Delta\eta)\frac{L+1}{4L} + r_t(r_1-\Delta\eta)\frac{L+1}{4L}\right\}\right]^2 \cdot \frac{RG}{4}. \tag{6}$$

Therefore, the CIR is given by

$$CIR_{odd}(r_t, r_1, r_2, L) = \left[\left\{(1-r_2\Delta\eta)L_{c1} + r_t\left(r_1-\Delta\eta\right)L_{c2}\right\} \Big/ \left\{\begin{array}{l}(1 - r_2\Delta\eta)L_{I1} + (r_1 - \Delta\eta)L_{I2} \\ \quad + r_t\left(1 - r_2\Delta\eta\right)L_{I3} + r_t\left(r_1 - \Delta\eta\right)L_{I4}\end{array}\right\}\right]^2 \tag{7}$$

$$= 4\left[\left\{(1+r_t r_1 - \Delta\eta\left(r_t+r_2\right))L + r_t r_1 - 1 - \Delta\eta\left(r_t - r_2\right)\right\} \Big/ \left\{\begin{array}{l}((1+r_t)(1+r_1) - \Delta\eta(1+r_t)(1+r_2))\,L \\ \quad -(1+r_t+r_t r_1 - 3r_1 - \Delta\eta(r_2+r_t r_2+r_t-3))\end{array}\right\}\right]^2. \tag{8}$$

Since the optical powers of both branches are balanced by a tuning optical attenuator, $\Delta\eta$ becomes approximately 1 for calculation. In the ideal case that the

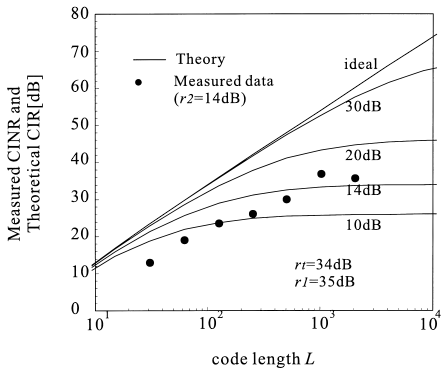

Fig. 7 Comparison of theoretical CIR and measured CINR.

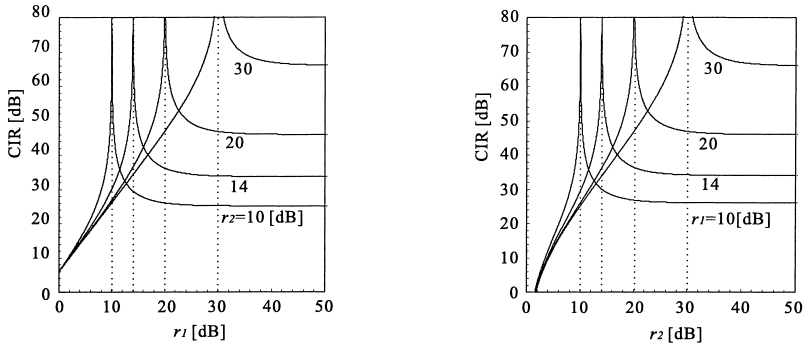

Fig. 8 Relationship between CIR_{odd} and r_1, r_2.

extinction ratios, r_t, r_1, and r_2 are infinitely large, CIR_{odd} becomes $\frac{L^2-2L+1}{4}$. For $L \to \infty$, on the other hand, CIR_{odd} is limited by the extinction ratios as

$$CIR_{odd}(r_t, r_1, r_2) = 4\left\{\frac{1 + r_t r_1 - r_t - r_2}{(1 + r_t)(r_1 - r_2)}\right\}^2. \quad (9)$$

Equation (9) shows that CIR_{odd} becomes infinitely large when the r_1 and r_2 are balanced except for the case of r_t=1. In this exceptional case of r_t=1, Eq. (9) becomes 1, and it is the critical situation for the received CIR performance. Assuming that the extinction ratio, r_t, is infinitely large, Eq. (9) becomes simply written by

$$CIR_{odd}(r_t = \infty, r_1, r_2) = 4\left(\frac{1 - r_2}{r_1 - r_2}\right)^2. \quad (10)$$

From the numerator of this equation, the desired RF power is related to the extinction ratio, r_2, and from the denominator of this equation, the interference RF power is related to the imbalance of the extinction ratio, $|r_1$-$r_2|$.

Figure 7 shows the comparison between measured CINR and theoretical CIR_{odd} considering the degradation of the extinction ratio. In this figure, the measured CINR was obtained under the condition that (r_t,r_1,r_2) were (34,35,14) [dB]. Theoretical CIR_{odd} performance is calculated from Eq. (8) for the extinction ratio, r_t and r_1 of 34 dB and 35 dB, respectively, which are the same as the values in the experiment. In the figure, the ideal condition is that all the extinction ratios are infinitely large. It is seen from Fig. 7 that the slope in the improvement of measured CINR with increased L was less than that in the theoretical ideal case. The theoretical result of CIR_{odd} for $r_2 = 14$ dB illustrates that this degradation in the slope is due to the extinction ratio lack in the lower side branch. For large L, the measured CINR was saturated at about 30 dB. The reason for this phenomena is evident from the theoretical result, Eq. (10)

Here, we theoretically examine in detail the influence from the extinction ratio in CIR_{odd}.

Figure 8 shows the relationship between CIR and

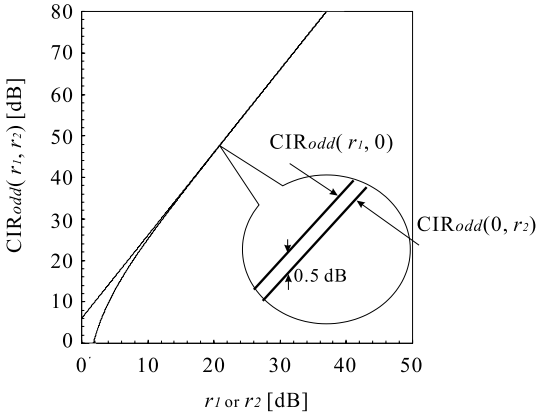

Fig. 9 Comparison of $CIR_{odd}(r_1, r_2 = 0)$ and $CIR_{odd}(r_1 = 0, r_2)$.

r_1 or r_2. The CIR values are saturated as large r_1 or r_2, and the value is $4(1/r_2 - 1)^2$ or $4(1/r_1)^2$, respectively.

Figure 9 shows the comparison of $CIR_{odd}(r_1, 0)$ and $CIR_{odd}(0, r_2)$. $CIR_{odd}(r_1, 0)$ is slightly larger than $CIR_{odd}(0, r_2)$. In this experiment, the extinction ratios of the upper side and lower side in receivers, r_1 and r_2, are about 34 dB and 14 dB, respectively. Thus, trading upper side optical switch and lower side optical switch improves CIR by about 0.5 dB. In the case of using a single switch decoder, CIR_{odd} is converged to 6 dB, by setting r_1 to be infinitely great and r_2 to be 0. This matches the experimental result shown in Fig. 5.

5. CIR Improvement Method

In the DOS CDM system, there are two methods of code mapping onto the optical on-off pulses; the even '1' symbols in a M-sequence (we assume that the number of '1's is even) are allocated to the optical On-pulses, or the odd '0' symbols in a M-sequence (we assume that the number of '0's is odd) are allocated to the optical On-pulses. By allocating even '1' symbols in the On-pulses of the IM/CDM signal format, we will be able to construct an interference-free DOS CDM RoF system. In addition, we experimentally examine its CIR improvement.

5.1 Orthogonal M-Sequence Multiplex Transmission

Assume that M IM/CDM signals are transmitting to each RBSs from CS. Each spreading code is synchronized, and then used to encode the RF signals. Bit-shifted M-sequences are allocated to each spreading code, $\boldsymbol{c}$= $\{c_0,\ c_1,\ \cdots,\ c_k,\ \cdots,\ c_{L-1}\}$= $\{\boldsymbol{a},\ T\boldsymbol{a},\ \cdots,\ T^k\boldsymbol{a},\ \cdots,\ T^{L-1}\boldsymbol{a}\}$ are used as a code for multiplexing, where T is the chip delay operator and $\boldsymbol{a}$ is one M-sequence with the code length of L. Therefore, L channels are applicable to the downlink. LD is directly modulated by the k-th RF signal, $g_k(t)$, with the optical modulation index of 1. Direct Optical Switching is performed at an OSW driven with a $\{0,\ 1\}$-valued M-sequence, c_k. We assume that the desired M-sequence is $c_k = T^k\boldsymbol{a}$, and the undesired ones are $c_m = T^m\boldsymbol{a}$, $(m \neq k, 0 \leq m \leq (M-1))$. Then, the intensities of the optical signal to k-th RBS, I_k, and the multiplexed optical signal, I, at the output of CS, are given by

$$\begin{aligned} I_k &= P_S(1+g_k(t))\cdot c_k, \\ I &= \sum_{m=0}^{M-1} P_r(1+g_m(t))\cdot c_m, \end{aligned} \tag{11}$$

where P_S is the peak transmitted laser power and $g_k(t)$ is the RF signal. P_r is the received optical power given by P_S/F_{loss}, where F_{loss} is the optical loss between CS and each of the RBSs. We assume that an optical amplifier (OA) is equipped at each RBS and the gain of each OA is equal to F_{loss}, thus P_S is equal to P_r. At a BMPD in the OPRC, the output currents i and i_n are given by

$$i = \sum_{m=0}^{M-1} \alpha P_r g_m(t) c_m \cdot \chi(c_k), \tag{12}$$

$$i_n = \alpha P_r \left\{ \sum_{m=0}^{M-1} g_m(t) c_{mn} \right\} \cdot \chi(c_{kn}), \tag{13}$$

where α is sensitivity of the BMPD, and n is the chip number of the spreading code. $\{+1, -1\}$-valued sequence, $\chi(c_{kn})$=$2c_{kn}-1$. The crosscorrelation function between ϕ_n=$\sum_{m=0}^{M-1} c_{mn}$ and $\chi(c_{kn})$ is given by (see Appendix)

$$\begin{aligned} \hat{\theta}_{\phi,\chi(c_k)}(l) &= \sum_{n=0}^{L-1} \phi_{n+l}\cdot\chi(c_{kn}) \\ &= \sum_{n=0}^{L-1} \left\{ c_{k(n+l)} + \sum_{\substack{m=0 \\ \neq k}}^{M-1} c_{m(n+l)} \right\} \cdot \chi(c_{kn}). \end{aligned} \tag{14}$$

The cross-correlation value at $l = 0$ is,

$$\begin{aligned} \hat{\theta}_{\phi,\chi(c_k)}(0) &= \sum_{n=0}^{L-1} \left\{ c_{kn}\cdot\chi(c_{kn}) + \sum_{\substack{m=0 \\ \neq k}}^{M-1} c_{mn}\cdot\chi(c_{kn}) \right\} \\ &= \sum_{\{c_{kn}=1\}} (2c_{kn}-1) + \sum_{\substack{m=0 \\ \neq k}}^{M-1} \sum_{\{c_{mn}=1\}} (2c_{kn}-1) \\ &= 2\sum_{\{c_{kn}=1\}} c_{kn} - wt(c_k) \\ &\quad + \sum_{\substack{m=0 \\ \neq k}}^{M-1} \left\{ 2\sum_{\{c_{mn}=1\}} c_{kn} - wt(c_m) \right\} \\ &= wt(c_k) + \sum_{\substack{m=0 \\ \neq k}}^{M-1} \theta_{c_m,\chi(c_k)}(0), \end{aligned} \tag{15}$$

where $wt(c_k)$ denotes the Hamming weight of c_k, i.e., the number of 1's in c_k. $\theta_{c_m,\chi(c_k)}(l)$ denotes the cross-correlation function between the {0,1}-valued sequence, c_m, and the $\{-1, +1\}$-valued sequence, $\chi(c_k)$. Then (see Appendix)

$$\hat{\theta}_{\phi,\chi(c_k)}(0) = \begin{cases} \frac{L+1}{2} & \text{for } wt(c_k) = \frac{L+1}{2} \\ \frac{L-1}{2} - (M-1) & \text{for } wt(c_k) = \frac{L-1}{2} \end{cases}. \tag{16}$$

Since no interference component exists in the case of an even weight M-sequence, it is possible to construct an interference-free communication system.

5.2 Measurement and Theoretical Analysis of CINR

When applying M-sequence with its code length L and even weight, CIR is derived in the same manner as in Sect. 4 as

$$\begin{aligned} &CIR_{even}(r_t, r_1, r_2, L) \\ &= 4\left[\left\{ (1+r_t r_1 - \Delta\eta\,(r_t+r_2))L + 1 - r_t r_1 - \Delta\eta\,(r_2 - r_t) \right\} \right. \\ &\left. \Big/ \left\{ \begin{array}{l} ((1+r_t)(1+r_1) - \Delta\eta(1+r_t)(1+r_2))\,L \\ -(1+r_1+r_t r_1 - 3r_t - \Delta\eta(r_2+1+r_t-3r_2)) \end{array} \right\} \right]^2. \end{aligned} \tag{17}$$

We assume that $\Delta\eta$=1 and $r_t \to \infty$. CIR_{even} and CIR_{odd} become

$$CIR_{even}(r_1, r_2, L) = 4\left(\frac{1-r_2}{r_1-r_2}\right)^2, \tag{18}$$

$$CIR_{odd}(r_1, r_2, L) = 4\left\{ \frac{(1-r_2)(L-1)}{(r_1-r_2)L - 4 + r_1 + 3r_2} \right\}^2. \tag{19}$$

We also consider the noise power, N, which was measured as being around -105 dBm. We represent CINR improvement between $CINR_{even}$ and $CINR_{odd}$ by the

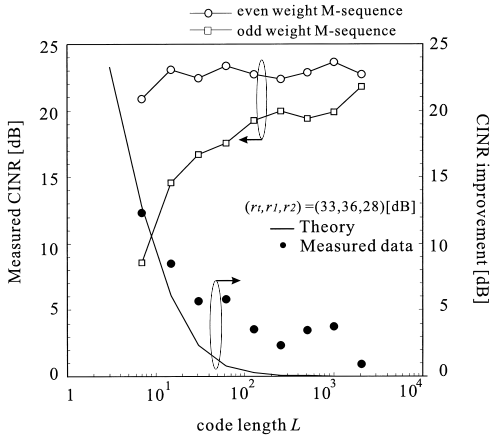

Fig. 10 Measured CINR and CINR improvement.

follow equation,

$$10\log\left(\frac{CINR_{even}(r_1,r_2,L)}{CINR_{odd}(r_1,r_2,L)}\right).\,[\mathrm{dB}]$$

Figure 10 shows the experimental result of measured CINR performance versus code length when using an even weight M-sequence compared to that when using an odd weight M-sequence. In this figure, the $CINR_{even}$ performance shows no change due to the code length, and was observed around 23 dB. It is evident that the $CINR_{even}$ is limited only receiver's noise power. There is a CIR improvement of 12 dB in the case of a code length of 7 chips compared to that with the odd weight M-sequence. In the case that the code length is 127 chips, a 4 dB CIR improvement is obtained.

The measured CIR improvement value becomes lower as the code length increases, because the extinction ratio limits the CINR performance. This phenomena is also confirmed theoretically with Eqs. (18) and (19), where $CINR_{odd}$ is approximated to $CINR_{even}$ under the condition of $L\to\infty$.

6. Conclusion

In this work, we experimentally demonstrated interference suppression in a Direct Optical Switching CDM Radio-on-Fiber System. The OPRC enables us to use M-sequence and Gold-sequence as codes for multiplexing, and the interference suppression effect is obtained by using OPRC instead of the single switch decoder. It is found that the CIR performance is deteriorated and saturated due to degradation of the extinction ratio of the optical switch. Furthermore, we observed that the CIR is improved by changing the code mapping method using the even weight M-sequence to one using the odd weight M-sequence. As a result of this experimental investigation of the total DOS CDM RoF system, the following were found:
(1) In the case of using OPRC, 13 dB CINR is obtained in the case that the code length is 31 chips, and 35 dB CINR is obtained in the case that the code length is 1023 chips. On the other hand, in the case of using a single switch decoder, we obtained no improvement even when the code length was increased, and its CINR was around 6 dB.
(2) It is found that the leak power occurs due to the degradation of the extinction ratio in the lower side branch. CIR performance saturation is observed in the region of the code length being long, that is, where the leak power limits the CIR performance.
(3) We obtained CINR improvement of 12 dB in the case of using an even weight M-sequence compared to using an odd weight M-sequence in the case of the code length of 7 chips. In the case that the code length is 127 chips, a 4 dB CIR improvement is obtained.

Acknowledgment

This paper is partially supported by the Grant-in-Aid for Scientific Research (B) No.14350202, from the Japan Society for the Promotion of Science.

References

[1] S. Komaki, K. Tsukamoto, S. Hara, and N. Morinaga, "Proposal of fiber and radio extension link for future personal communications," Microwave Opt. Technol. Lett., vol.6, no.1, pp.55–60, Jan. 1993.
[2] Y. Shoji, K. Tsukamoto, and S. Komaki, "Proposal of radio high-way networks using asynchronous time division multiple access," IEICE Trans. Commun., vol.E79-B, no.3, pp.308–315, March 1996.
[3] H. Harada, S. Kajiya, K. Tsukamoto, S. Komaki, and N. Morinaga, "TDM intercell connection fiber-optic bus link for personal radio communication system," IEICE Trans. Commun., vol.E78-B, no.9, pp.1287–1294, Sept. 1995.
[4] S. Kajiya, K. Tsukamoto, and S. Komaki, "Proposal of fiber-optic radio highway networks, using CDMA method," IEICE Trans. Electron., vol.E79-C, no.1, pp.111–117, Jan. 1996.
[5] S. Park, K. Tsukamoto, and S. Komaki, "Polarity-reversing type photonic receiving scheme for optical CDMA signal in radio highway," IEICE Trans. Electron., vol.E81-C, no.3, pp.462–467, March 1998.
[6] S. Park, K. Tsukamoto, and S. Komaki, "Proposal of direct switching CDMA for cable-to-the-air system and its perfomance analysis," IEICE Trans. Commun., vol.E81-B, no.6, pp.1188–1196, June 1998.
[7] K. Kumamoto, K. Tsukamoto, and S. Komaki, "Proposal of higher-order spread spectrum direct optical switching CDMA system," IEICE Trans. Commun., vol.E83-B, no.8, pp.1753–1765, Aug. 2000.
[8] S. Tamura, S. Nakano, and K. Okazaki, "Optical code-multiplex transmission by gold sequence," J. Lightwave Technol., vol.LT-3, pp.121–127, Feb. 1985.
[9] T. Shokawa, T. Higashino, K. Kumamoto, K. Tsukamoto, and S. Komaki, "Experimental demonstration of interference suppression with optical polarity-reversing correlator in DOS-CDMA radio-on-fiber networks," The 2nd Korea-Japan Joint Workshop on Microwave-Photonics, pp.55–58, Seoul, Korea, Feb. 2001.

[10] T. Higashino, K. Tsukamoto, and S. Komaki, "Experimental study of received signal performance in direct optical switching CDMA ROF system," Microwave-Photonics 2002, pp.233–236, Awaji, Japan, Nov. 2002.

Appendix: Cross-correlation Function in DOS CDM System

$u = \{u_0, u_1, \ldots, u_{L-1}\}$ or $v = \{v_0, v_1, \ldots, v_{L-1}\}$ denotes a {0,1}-valued sequence with length of L. $\chi(v) = \{\chi(v_0), \chi(v_1), \ldots, \chi(v_{L-1})\}$ denotes a $\{-1, +1\}$-valued sequence, where $\chi(\alpha) = 2\alpha - 1$ for $\alpha = 0$ or 1. We define that $\theta_{u,\chi(v)}(l)$ is a periodic cross-correlation function between {0,1}-valued sequence, u and $\{-1, +1\}$-valued sequence, $\chi(v)$. This cross-correlation function is given by [8]

$$\begin{aligned}\theta_{u,\chi(v)}(l) &= \sum_{i=0}^{L-1} u_i \cdot \chi(v_{i+l}) \\ &= \sum_{i=0}^{L-1} (u_i v_{i+l} - u_i \overline{v_{i+l}}) \\ &= \sum_{i=0}^{L-1} u_i v_{i+l} - \sum_{i=0}^{L-1} u_i \overline{v_{i+l}} \\ &= wt\left(uT^l v\right) - wt\left(uT^l \overline{v}\right), \end{aligned} \tag{A·1}$$

where $\overline{v}$ is the inverse of v (v= 0 or 1). Furthermore, $\theta_{u,\chi(v)}(l)$ can be rewritten as

$$\begin{aligned}\theta_{u,\chi(v)}(l) &= \sum_{i=0}^{L-1} u_i \cdot \chi(v_{i+l}) \\ &= \sum_{\{u_i=1\}} (2v_{i+l} - 1) \\ &= \sum_{\{u_i=1\}} 2v_{i+l} - \sum_{\{u_i=1\}} 1 \\ &= 2 \sum_{\{u_i=1\}} v_{i+l} - wt(u). \end{aligned} \tag{A·2}$$

Thus, from Eq. (A·2), we obtain

$$\sum_{\{u_i=1\}} v_{i+l} = \frac{1}{2}\left(\theta_{u,\chi(v)}(l) + wt(u)\right). \tag{A·3}$$

Let $\boldsymbol{a}$ and $\boldsymbol{b}$ denote an M-sequence with code length of L. Assume that $\boldsymbol{b}$=$T^\tau \boldsymbol{a}$ and $\tau \neq 0$. The cross-correlation value between $\boldsymbol{a}$ and $\boldsymbol{b}$ at the place without shift is given by

$$\begin{aligned}\theta_{a,\chi(b)}(0) &= wt(\boldsymbol{a} \cdot \boldsymbol{b}) - wt(\boldsymbol{a} \cdot \overline{\boldsymbol{b}}) \\ &= wt(\boldsymbol{a}T^\tau \boldsymbol{a}) - wt(\boldsymbol{a}T^\tau \overline{\boldsymbol{a}}) \\ &= \theta_{a,\chi(a)}(\tau). \end{aligned} \tag{A·4}$$

Therefore,

$$\theta_{a,\chi(a)}(\tau) = \begin{cases} wt(\boldsymbol{a}) & \tau = 0 \\ 0 & \tau \neq 0 \quad \text{and} \quad wt(\boldsymbol{a}) = \frac{L+1}{2} \\ -1 & \tau \neq 0 \quad \text{and} \quad wt(\boldsymbol{a}) = \frac{L-1}{2} \end{cases}. \tag{A·5}$$

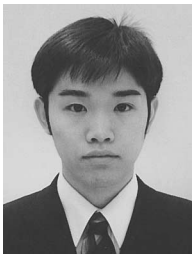

Takeshi Higashino was born in Osaka, Japan on November 11, 1978. He received the B.E. and M.E. degrees in Communications Engineering from Osaka University, Osaka, Japan, in 2001 and 2002, respectively. He is currently pursuing the Ph.D. degree at Osaka University. He is engaged in the research on radio and optical communication systems.

Katsutoshi Tsukamoto was born in Shiga, Japan on October 7, 1959. He received the B.E., M.E. and Ph.D. degrees in Communications Engineering from Osaka University in 1982, 1984 and 1995, respectively. He is currently an Associate Professor in the Department of Communications Engineering at Osaka university, engaged in research on radio optical communication systems. He is a member of IEEE and ITE. He was awarded the Paper Award of IEICE, Japan in 1996.

Shozo Komaki was born in Osaka, Japan in 1947. He received the B.E., M.E. and Ph.D. degrees in Communications Engineering from Osaka University in 1970, 1972 and 1983, respectively. In 1972, he joined the NTT Radio Communication Labs., where he has engaged in repeater development for a 20-GHz digital radio system, and 16-QAM and 256-QAM systems. In 1990, he moved to Osaka University, Faculty of Engineering, and is engaged in research on radio and optical communication systems. He is currently a Professor of Osaka University. Dr. Komaki is a senior member of the Institute of Television Engineering of Japan (ITE). He was awarded the Paper Award and the Achievement Award of IEICE, Japan, in 1977 and 1994, respectively.